

BIROn - Birkbeck Institutional Research Online

Crawford, Ian (2002) Detection of CaI and CH absorption at the velocity of the variable interstellar component towards Velorum. *Monthly Notices of the Royal Astronomical Society* 334 (2), L33-L37. ISSN 0035-8711.

Downloaded from: <https://eprints.bbk.ac.uk/id/eprint/28476/>

Usage Guidelines:

Please refer to usage guidelines at <https://eprints.bbk.ac.uk/policies.html> or alternatively contact lib-eprints@bbk.ac.uk.

Detection of Ca I and CH absorption at the velocity of the variable interstellar component towards κ Velorum

I. A. Crawford[★]

Department of Physics and Astronomy, University College London, Gower Street, London WC1E 6BT

Accepted 2002 May 31. Received 2002 May 31; in original form 2002 May 2

ABSTRACT

I report the detection of interstellar Ca I and CH at the velocity of the previously reported variable absorption component towards κ Velorum (HD 81188). The very high spectral resolution ($R \approx 900\,000$) has resolved the intrinsic line profiles, yielding a kinetic temperature of $T_k = 190_{-150}^{+170}$ K, and a line-of-sight turbulent velocity of $v_t = 0.26_{-0.13}^{+0.08}$ km s $^{-1}$, for the densest material. The Ca I/Ca II ratio implies a spatial density of $n_H \gtrsim 10^3$ cm $^{-3}$, although this may considerably underestimate the density in the variable region itself. The CH column density suggests a path-length of $\sim 10^2$ to 10^3 au, supporting suggestions that variable interstellar components such as this are formed in extended structures (sheets or filaments) aligned with the line of sight.

Key words: stars: individual: κ Vel (HD 81188) – ISM: structure.

1 INTRODUCTION

One of the most surprising recent developments in the study of the interstellar medium (ISM) has been the discovery of time-variable interstellar absorption lines (e.g. Blades et al. 1997; Price, Crawford & Barlow 2000; Crawford et al. 2000; Lauroesch, Meyer & Blades 2000; Welty & Fitzpatrick 2001; Danks et al. 2001). The time-scale of variation (years to decades) implies spatial structure on a 10–100 astronomical unit (au) scale.

In an earlier paper (Crawford et al. 2000, hereinafter Paper I) we presented evidence that the interstellar K I $\lambda 7698$ resonance line towards the bright, lightly reddened [$E(B - V) = 0.11$], southern star κ Velorum increased in strength by ~ 40 per cent between 1994 and 2000. A smaller (~ 16 per cent) increase was also observed in the Na I D₁ $\lambda 5896$ line. Based on the distance (165 ± 13 pc: ESA 1997) and proper motion of the star, the inferred spatial scale of the structure(s) responsible was $\lesssim 15$ au (Paper I). Of course, any significant transverse cloud velocity would increase the size estimate somewhat, but an exceptionally high velocity (~ 100 km s $^{-1}$) would be required to yield a spatial scale estimate as large as 100 au.

In order to explain comparably small-scale structures detected at radio wavelengths, Heiles (1997) has argued that the variable absorption occurs in cold ($T \sim 15$ K) and dense ($n_H \sim 10^3$ cm $^{-3}$) sheets or filaments embedded within warmer, less dense material. When such structures are aligned along the line of sight it is possible to achieve large variations in column density over small transverse scales, without requiring implausibly high spatial densities. Other possibilities for the formation of small, dense structures in the ISM include: fractal structures arising from turbulence (e.g. Elmegreen

1999); a hypothesized population of small, self-gravitating clodlets (e.g. Draine 1998; Wardle & Walker 1999); and structures generated by the slow-mode magnetohydrodynamic (MHD) waves recently discussed by Falle & Hartquist (2002).

To distinguish between these various possibilities, further information on the physical conditions (especially the density) prevailing within the absorbing structures is required. With this in mind, I here report the results of a search for Ca I and CH at the velocity of the previously identified variable absorption component towards κ Vel. As described below, both these species were detected, yielding information on the physical conditions and molecular state of the absorbing material. The location of the interstellar absorption towards κ Vel was discussed by Dunkin & Crawford (1999), who concluded that it is probably associated with the ‘ridge’ of molecular clouds which dominate the ISM in the fourth Galactic quadrant for distances $\gtrsim 150$ pc (cf. fig. 7 of Dame et al. 1987). While this would place the absorption relatively close to the star, there is no compelling evidence for a physical association between them, and the small linewidths (Section 4.1) are indicative of the cold, undisturbed ISM.

2 OBSERVATIONS

Observations of the Ca I (4226.728 Å) and CH R₂(1) (4300.313 Å) lines were obtained using the Ultra-High-Resolution Facility (UHRF: Diego et al. 1995) at the Anglo-Australian Telescope (AAT) in 2002 March. New observations of the Ca II K (3933.663 Å) and K I (7698.974 Å) lines were also obtained, for comparison with earlier observations. A list of the individual observations is given in Table 1. Measurement of a stabilized He–Ne laser line indicated an instrumental resolution of 0.330 ± 0.012 km s $^{-1}$, or a

[★]E-mail: iac@star.ucl.ac.uk

Table 1. Summary of the observational data. Exp. is the exposure time (number of exposures times the integration time of each); SNR is the continuum signal-to-noise ratio; and $W_\lambda(\text{tot})$ is the total equivalent width (2σ errors).

Line	UT date	Exp. ($n \times s$)	SNR	$W_\lambda(\text{tot})$ (mÅ)
Ca I	01-03-02	3×1800	170	0.90 ± 0.08
Ca II	01-03-02	1×1800	100	16.70 ± 0.28
K I	03-03-02	1×1800	90	4.21 ± 0.26
CH	02-03-02	7×1800	400	0.21 ± 0.04

resolving power $R (\equiv \lambda / \Delta \lambda) = 9.1 \times 10^5$. The detector was an EEV CCD (2048 × 4096 13.5-μm pixels), orientated with its long sides parallel to the echelle dispersion. As usual, an image-slicer was used (Diego 1993), and the CCD was binned by a factor of eight in the cross-dispersion direction to reduce the readout noise. Even with this binning, the spectra cover ~ 130 binned pixels in the cross-dispersion direction, making the extracted spectra quite insensitive to pixel-to-pixel sensitivity variations. This sensitivity was further reduced by moving the grating angle slightly between the multiple observations of the weak Ca I and CH lines, thus ensuring that the lines fell on different areas of the detector. Moreover, all the spectra were divided by a flat-field; this was provided by a quartz-halogen lamp for the blue (Ca I, Ca II and CH) lines, but for the K I region division by the spectrum of a bright early-type star (β Cen) was found to correct better for CCD fringing and telluric water lines.

The spectra were extracted from the CCD images using the FIGARO data reduction package (Shortridge et al. 1998), and subsequent manipulations and measurements were performed using the

DIPSO spectral analysis package (Howarth et al. 1998), at the University College London Starlink node. Detector and instrumental (scattered light) backgrounds were measured from the inter-order region and subtracted. The spectra were wavelength-calibrated using a Th–Ar comparison lamp, and then converted to a heliocentric velocity scale. The multiple integrations of Ca I and CH were then co-added. The resulting spectra are shown in Fig. 1.

3 LINE PROFILE ANALYSIS

The observed line profiles were modelled using a χ^2 -minimization routine, VAPID (Howarth et al. 2002). This program returns the optimum values of column density (N), velocity dispersion (b) and central heliocentric velocity (v_{helio}) for a specified number of absorption components, and these values are given in Table 2. The rest wavelengths and oscillator strengths were taken from Morton (1991) for the atomic lines, and from Black & van Dishoeck (1988) for CH. The CH R₂(1) line is split into a Λ-doublet (separated by 1.43 km s⁻¹), while the K I line exhibits hyperfine structure with a separation of 0.35 km s⁻¹ (Welty, Hobbs & Kulkarni 1994). The former is clearly resolved by the UHFR, while the latter is comparable to the instrumental resolution; both have been allowed for in the analysis, and the quoted heliocentric velocities are with respect to the weighted mean central velocities.

As discussed in Paper I, there is fairly convincing evidence that the main Na I velocity component towards this star actually consists of two unresolved subcomponents separated by ~ 0.25 km s⁻¹. Given the similar ionization and depletion properties of Na I and K I, this structure was also assumed in the K I analysis presented in Paper I. However, given that there is no convincing evidence for this substructure in the present data, and that at least some of these lines

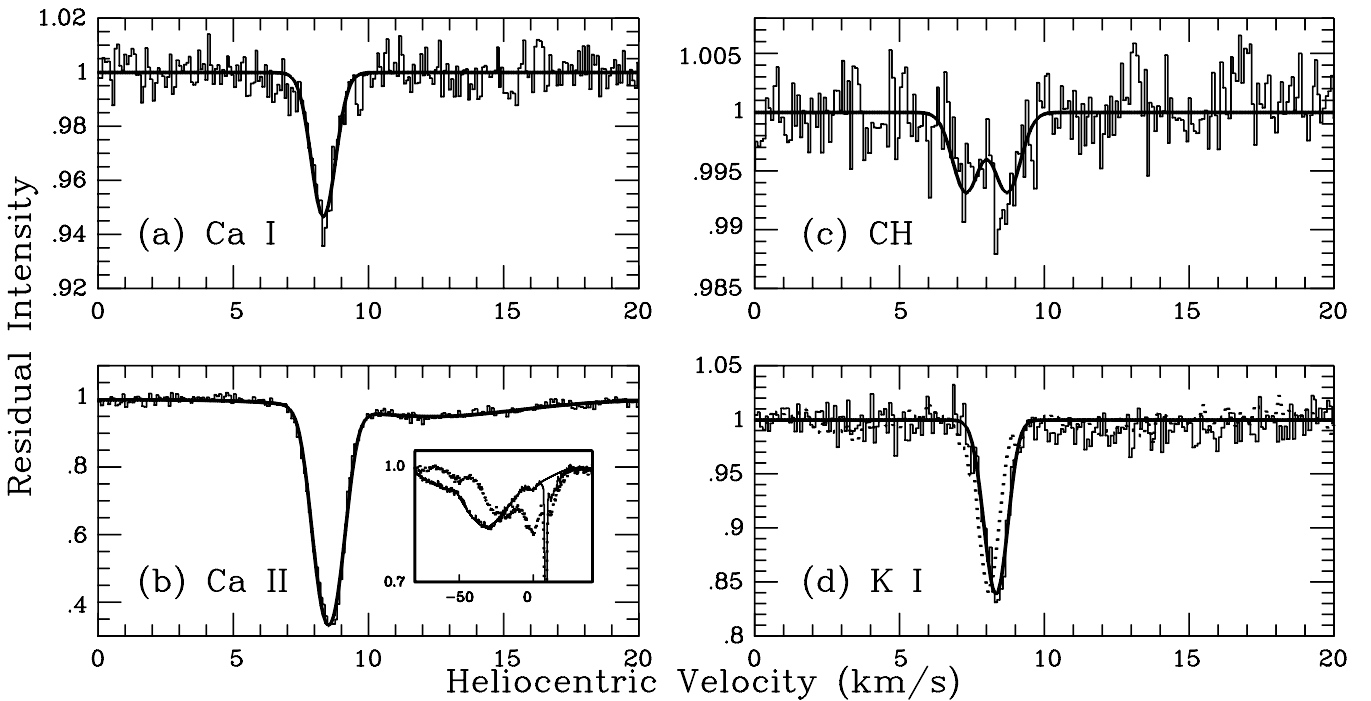


Figure 1. The interstellar lines observed towards κ Vel. The observed data are plotted as histograms, and the best-fitting theoretical profiles (characterized by the parameters given in Table 2) are overplotted. The inset in (b) shows the change in the underlying stellar spectrum between 1994 (dots) and 2002 (histogram) owing to the spectroscopic binary nature of the star; the spline fit here used to approximate the stellar profile is shown as a solid line. The dotted profile in (d) shows the 2000 March K I profile for comparison with the 2002 result (the ~ 0.2 km s⁻¹ velocity difference most likely results from wavelength calibration uncertainties).

Table 2. Results of the line profile analysis: v_{helio} , b and $\log N$ are the heliocentric velocity, velocity dispersion and column density (1σ errors). The resulting line profiles are compared with the observations in Fig. 1. T_k^{ul} gives the rigorous upper limit to the kinetic temperature based on the observed b -value (i.e. assuming that there is no ‘turbulent’ contribution to the linewidth; see text).

Line	v_{helio} (km s $^{-1}$)	b (km s $^{-1}$)	$\log N$ (cm $^{-2}$)	T_k^{ul} (K)
Ca I	8.34 ± 0.03	0.59 ± 0.04	9.50 ± 0.02	840 ± 120
Ca II	8.54 ± 0.01	0.66 ± 0.01	11.30 ± 0.01	1050 ± 30
	12.34 ± 0.22	4.52 ± 0.28	10.79 ± 0.03	–
K I	8.30 ± 0.02	0.46 ± 0.03	10.40 ± 0.02	500 ± 65
CH	8.01 ± 0.08	0.61 ± 0.09	11.43 ± 0.04	290 ± 90

may form in different regions, I have here modelled this feature as a single velocity component. There is clear evidence for additional weak Ca II absorption extending to $v_{\text{helio}} \sim +18$ km s $^{-1}$, which is also present in Na I (Dunkin & Crawford 1999) and possibly K I (note the low continuum over this velocity range in Fig. 1d). Because the local continuum is poorly defined (owing to the uncertain underlying stellar spectrum, see below), this has been modelled here as a single broad ($b \sim 4.5$ km s $^{-1}$) component, although several discrete velocity components are probably present (cf. Dunkin & Crawford 1999).

4 DISCUSSION

4.1 The linewidths

It is noteworthy that the lines at the velocity of the ‘main’ (variable) component are all very narrow ($b < 1$ km s $^{-1}$; Table 2). Although narrow, all of these lines have been fully resolved by the UHRF (the instrumental b -value being $0.330/1.6651 = 0.20$ km s $^{-1}$), and have been fully sampled (note the ~ 0.1 km s $^{-1}$ pixel size in Fig. 1). The measured linewidths are therefore reliable, and may be used to place constraints on the prevailing physical conditions.

The primary line-broadening mechanisms in the neutral interstellar medium are thermal Doppler broadening, and broadening arising from bulk motions of the gas (‘turbulence’). These combine to produce the observed b -values, as follows:

$$b = \sqrt{\frac{2kT_k}{m_A} + 2v_t^2}, \quad (1)$$

where T_k is the kinetic temperature, v_t is the rms line-of-sight turbulent velocity, k is Boltzmann’s constant, and m_A is the mass of the element (atomic mass A) under observation. By putting $v_t = 0$ in equation (1) it is possible to obtain a rigorous upper limit to the kinetic temperature, T_k^{ul} , and these values are listed in Table 2. Of course, the actual kinetic temperatures are likely to be much lower.

Note that the Ca II b -value is significantly larger than that of K I, whereas equation (1) indicates $0.987 \leq b(\text{Ca II})/b(\text{K I}) \leq 1.0$ (owing to their near-identical atomic masses). This is a clear indication that the Ca II has formed in a warmer and/or more turbulent region, presumably in an outer envelope. This effect is well known in studies of diffuse interstellar clouds (e.g. Crinklaw, Federman & Joseph 1994; Barlow et al. 1995), but its most important implication here is that Ca II may not trace the densest regions responsible for the observed variations in K I and Na I.

Interestingly, there is some indication that the Ca I line is narrower than that of Ca II, although formally this is barely significant

given the errors. As Ca I is likely to form preferentially in denser regions (owing to enhanced recombination) such a result is not unexpected – and it may be noted that the Ca I b -value is intermediate between those of Ca II and K I. Clearly, if Ca I and Ca II do indeed trace different regions, this has important consequences for the interpretation of the Ca ionization balance discussed below.

A final item of physical information can be obtained from equation (1) if we assume that the CH and K I lines both arise in the densest, variable region. Because these two species have very different masses (13 and 39 amu, respectively) it is possible to solve equation (1) simultaneously for both T_k and v_t . This yields $T_k = 190^{+170}_{-150}$ K and $v_t = 0.26^{+0.08}_{-0.13}$ km s $^{-1}$. A similar temperature (270^{+480}_{-220} K) was obtained by Dunkin & Crawford (1999) from a comparison of the K I and Na I linewidths – although of course if, as discussed in Section 3, two unresolved subcomponents contribute to the profiles, the value of T_k in each could be lower (cf. table 4 of Dunkin & Crawford 1999, also the b -values listed in table 2 of Paper I, which imply $T_k \lesssim 100$ K for the narrowest subcomponent). Although the errors on these temperature estimates are quite large, they do suggest that T_k in the variable region may not be as low as the 15 K advocated by Heiles (1997). Clearly, spectra of higher signal-to-noise ratio, especially of CH, are desirable to confirm this.

4.2 The Ca ionization balance

As can be seen in Fig. 1(a), a solid detection of Ca I has been obtained. Although weak ($W_\lambda = 0.90 \pm 0.08$ mÅ; Table 1), the strength of this line is nevertheless unusual for a star of such low reddening. Indeed I am unaware of any reported Ca I detection for a star with an $E(B - V)$ as low as 0.11, although Penprase (1993) did find one case (HD 89688) with $E(B - V) = 0.16$ and $W_\lambda(\text{Ca I}) = 2.0$ mÅ. Of previous Ca I detections (e.g. Lambert & Danks 1986; Grede, van Dishoeck & Black 1993; Penprase 1993; Allen 1994), only Lambert & Danks identified cases with sub-mÅ equivalent widths, and the six stars with line strengths similar to that of κ Vel [$0.6 \leq W_\lambda(\text{Ca I}) \leq 1.2$ mÅ] all have colour excesses at least twice as large [$0.20 \leq E(B - V) \leq 0.37$; median value: 0.24].

The Ca I detection may be combined with that of Ca II to estimate the electron density in the absorbing medium. Ca II was re-observed here, to check for variability since the last published spectrum was obtained in 1994 (Dunkin & Crawford 1999). This comparison is complicated by the fact that κ Vel is a spectroscopic binary, and the photospheric lines, which form the local continuum for the interstellar lines, have changed considerably between the two observations (as shown in the inset in Fig. 1b). However, there is no compelling evidence for a change in the interstellar Ca II line between 1994 and 2002. This is not necessarily inconsistent with the changes reported for Na I and K I in Paper I, because, as discussed in Section 4.1, Ca II most likely arises in a different, presumably more extended, region.

Assuming for the moment that the Ca I and Ca II lines sample the same material (but bearing in mind the caveat introduced above that they may not), and that an equilibrium holds between photoionization and recombination, the electron density, n_e , is given by

$$n_e = \frac{N(\text{Ca I})}{N(\text{Ca II})} \times \frac{\Gamma}{\alpha}, \quad (2)$$

where Γ is the Ca I photoionization rate, and α is the recombination coefficient from Ca II to Ca I. Taking the photoionization rates from van Dishoeck (1988, assuming the unattenuated Draine (1978) radiation field), and the recombination rates of Péquignot & Aldrovandi (1986), we obtain $n_e = 0.97$ cm $^{-3}$ for a temperature of 100 K [falling to 0.27 cm $^{-3}$ at the Heiles (1997) preferred value of 15 K]. These are

very high values for the diffuse interstellar medium (see e.g. Grede et al. 1993), and suggest either an unusual degree of H ionization or a high spatial density. Indeed, assuming that the free electrons arise predominantly from the photoionization of carbon, a hydrogen density in the range 10^3 to 10^4 cm^{-3} is implied, depending on the carbon depletion.

If we adopt the (seemingly fairly constant) interstellar *gas-phase* C abundance of $n_C \sim 1.4 \times 10^{-4} n_H$ determined by Sofia et al. (1997, implying that ~ 60 per cent of the total C is locked into a solid phase), we obtain $n_H \sim 7 \times 10^3 \text{ cm}^{-3}$ at $T = 100 \text{ K}$ (or $2 \times 10^3 \text{ cm}^{-3}$ at 15 K). In principle, cosmic ray ionization of hydrogen would reduce these density estimates somewhat, but application of equation (5–32) of Spitzer (1978) indicates that this reduction amounts to only ~ 10 per cent given the cosmic ray ionization rate ($5 \times 10^{-17} \text{ s}^{-1}$) adopted by van Dishoeck & Black (1986) for nearby diffuse clouds. Even if we make the unlikely assumption that carbon is wholly undepleted with respect to the solar abundance (Anders & Grevesse 1989), we still obtain $n_H \sim 2.5 \times 10^3 \text{ cm}^{-3}$ for $T = 100 \text{ K}$ (or 700 cm^{-3} at 15 K). These density estimates ($n_H \gtrsim 10^3 \text{ cm}^{-3}$) are all consistent with those predicted by Heiles (1997) for his proposed filamentary structures.

Note, however, that these values are likely to *underestimate* the density of that part of the sightline responsible for the spectral variations observed in Na I and K I. If, as discussed in Section 4.1, the Ca II is largely contributed by an outer envelope of some kind, the Ca I/Ca II ratio, and hence the density, of the variable region will be greater than implied by the overall column densities given in Table 2.

4.3 The CH abundance

If the structures responsible for the variable interstellar lines are as cold and dense as suggested by Heiles (1997), we would expect the formation of simple diatomic molecules through the normal processes of interstellar gas-phase chemistry (e.g. Duley & Williams 1984). The present detection of CH is a vindication of this expectation, and a simple calculation indicates that the observed column density is of the expected order of magnitude.

The dominant route to CH in diffuse molecular clouds is through the ion–molecule reaction



with approximately 70 per cent of the CH_2^+ eventually forming CH (e.g. Federman 1982). The main destruction routes are photodissociation and reaction with C^+ , although the former dominates in regions of low extinction and $n_H \lesssim 10^4 \text{ cm}^{-3}$. Thus the equilibrium space density of CH is given by

$$n(\text{CH}) \approx \frac{0.7 \times k_3 \times n(\text{C}^+) \times n(\text{H}_2)}{k_{\text{pd}}(\text{CH})}, \quad (4)$$

where k_3 is the rate coefficient of equation (3) and $k_{\text{pd}}(\text{CH})$ is the CH photodissociation rate. Taking $k_3 = 4.0 \times 10^{-16} (T_k/300 \text{ K})^{-0.2} \text{ cm}^3 \text{ s}^{-1}$ (Millar, Farquhar & Willacy 1997), $k_{\text{pd}}(\text{CH}) = 9.5 \times 10^{-10} \text{ s}^{-1}$ (van Dishoeck 1988) and $n(\text{C}^+) = 1.4 \times 10^{-4} \times n_H$ (as above), we obtain the following expression for the CH column density (for $T_k = 100 \text{ K}$):

$$N(\text{CH}) \approx 400 \times f \times n_H^2 \times D_{\text{au}}, \quad (5)$$

where f is the fraction of hydrogen nuclei in H_2 molecules [i.e. $n(\text{H}_2) = f n_H/2$], and D_{au} is the path-length measured in au. [$N(\text{CH})$ would be ~ 50 per cent larger at $T_k = 15 \text{ K}$.]

It follows from equation (5) that, for a modest H_2 fraction (say $f \sim 0.1$) and a density $n_H \sim 2500 \text{ cm}^{-3}$ (consistent with the Ca I results), a path-length $D \sim 1000 \text{ au}$ is able to reproduce the CH column density observed here. Given that the *transverse* spatial scale of the absorbing structure (as implied by the variability time-scale) is $\sim 15 \text{ au}$, this suggests that we are indeed viewing an elongated structure such as the edge-on sheets or filaments proposed by Heiles (1997). Clearly, a higher density (and/or less extreme C depletion, larger f , or non-zero extinction) would reduce the path-length requirement, and thus the degree of elongation required. Heiles himself favoured extension factors of ~ 10 (i.e. path-lengths $\sim 100 \text{ au}$), which could be achieved here with e.g. $n_H \sim 5000 \text{ cm}^{-3}$ and $f \sim 0.25$. Note that molecular hydrogen fractions of $f \gtrsim 0.1$ are expected for $n_H \gtrsim 10^3 \text{ cm}^{-3}$, even for very low extinction [cf. models 3 and 4 due to Black (1975) and reproduced in fig. 5 of Savage et al. (1977)], provided that a sufficient H_2 column density ($\gtrsim 10^{15} \text{ cm}^{-2}$) develops to permit self-shielding of the molecule (Black, private communication).

4.4 The new K I observation

The main interest in this new observation is to see if K I continued to strengthen after 2000, given that its strength increased by 40 per cent between 1994 and 2000 (Paper I). Fig. 1(d) shows the 2000 March observation as a dotted line overplotted on the 2002 March spectrum, and the latter will be seen to be slightly (~ 6 per cent) deeper than the former. In order to determine if this small difference is at least consistent with the column density increasing at the 1994–2000 rate, new fits to the earlier spectra were performed (where, for consistency, I have now assumed a single velocity component in each case: cf. Section 3). This yielded the following logarithmic K I column densities: 10.21 ± 0.02 (1994 June) and 10.36 ± 0.02 (2000 March). These may be compared with the 10.40 ± 0.02 reported here (2002 March). Thus, while it is true that the 2002 value is barely different from the 2000 value given the errors, a trend is nevertheless apparent. The first pair of observations were separated by 5.75 yr , implying an average column density increase of $0.12 \times 10^{10} \text{ cm}^{-2} \text{ yr}^{-1}$. Extrapolated forward for two years, this would then predict a value of $2.53 \times 10^{10} \text{ cm}^{-2}$ ($\log N = 10.40$) for 2002 March, which is the observed value. Thus, while the temporal baseline is too short, and the errors too large, to be definitive, the 2002 data are at least consistent with the K I line continuing to increase in strength at the 1994–2000 rate. Clearly, continued monitoring of this line is warranted.

5 CONCLUSIONS

The main conclusions of this paper are as follows.

- (i) Lines arising from Ca I and CH have been detected at the velocity of the previously identified variable absorption component towards κ Vel, enabling information on the physical and chemical environment to be derived.
- (ii) New observations of Ca II and K I have also been obtained, and, while the Ca II line did not vary between 1994 and 2002, the K I data (Section 4.4) are consistent with a column density increase between 2000 and 2002 at the 1994–2000 rate.
- (iii) Analysis of the linewidths (Section 4.1) indicates that the non-variable Ca II line arises in a different (warmer and/or more turbulent) region than the variable K I line, probably in an extended envelope of some kind. Assuming that the K I and CH lines both trace the densest (variable) region, their b -values yield a temperature

of $T_k = 190^{+170}_{-150}$ K. This may exclude a temperature as low as the 15 K favoured by Heiles (1997), but observations at higher signal-to-noise ratio are needed to confirm this.

(iv) Analysis of the Ca I/Ca II ionization balance (Section 4.2) suggests a total hydrogen density of $\gtrsim 10^3$ cm $^{-3}$, assuming that these two lines have formed in the same region. However, given the evidence (Section 4.1) for different spatial locations of these species, this probably *underestimates* the density within the variable region itself.

(v) The observed CH abundance is also consistent with $n_H \gtrsim 10^3$ cm $^{-3}$ (Section 4.3). The CH column density then suggests path-lengths of $\sim 10^2$ – 10^3 au. As the transverse scale (estimated from the K I variability time-scale) is ~ 15 au, this supports the suggestion that variable interstellar lines are formed in extended structures (e.g. sheets or filaments) viewed end-on, as first suggested by Heiles (1997).

ACKNOWLEDGMENTS

I thank PPARC for an Advanced Fellowship, and PATT for telescope time. I am grateful to D. A. Williams and T. Nguyen for conversations on the CH abundance, S. R. Federman for pointing me to previous observations of Ca I, and J. H. Black for correspondence on the fractional abundance of H₂.

REFERENCES

- Allen M. M., 1994, ApJ, 424, 754
 Anders E., Grevesse N., 1989, Geochim. Cosmochim. Acta, 53, 197
 Barlow M. J., Crawford I. A., Diego F., Dryburgh M., Fish A. C., Howarth I. D., Spyromilio J., Walker D. D., 1995, MNRAS, 272, 333
 Black J. H., 1975, PhD thesis, Harvard University
 Black J. H., van Dishoeck E. F., 1988, ApJ, 331, 986
 Blades J. C., Sahu M. S., He L., Crawford I. A., Barlow M. J., Diego F., 1997, ApJ, 478, 648
 Crawford I. A., Howarth I. D., Ryder S. D., Stathakis R. A., 2000, MNRAS, 319, L1 (Paper I)
 Crinklaw G., Federman S. R., Joseph C. L., 1994, ApJ, 424, 748
 Dame T. M. et al., 1987, ApJ, 322, 706
 Danks A. C., Walborn N. R., Vieira G., Landsman W. B., Gales J., García B., 2001, ApJ, 547, L155
 Diego F., 1993, Appl. Opt., 32, 6284
 Diego F. et al., 1995, MNRAS, 272, 323
 Draine B. T., 1978, ApJS, 36, 595
 Draine B. T., 1998, ApJ, 509, L41
 Duley W. W., Williams D. A., 1984, Interstellar Chemistry. Academic Press, London
 Dunkin S. K., Crawford I. A., 1999, MNRAS, 302, 197
 Elmegreen B. G., 1999, ApJ, 527, 266
 ESA, 1997, The *Hipparcos* and Tycho Catalogues, ESA SP-1200
 Falle S. A. E., Hartquist T. W., 2002, MNRAS, 329, 195
 Federman S. R., 1982, ApJ, 257, 125
 Gredel R., van Dishoeck E. F., Black J. H., 1993, A&A, 269, 477
 Heiles C., 1997, ApJ, 481, 193
 Howarth I. D., Murray J., Mills D., Berry D. S., 1998, Starlink User Note, 50.21
 Howarth I. D., Price R. J., Crawford I. A., Hawkins I., 2002, MNRAS, in press
 Lambert D. L., Danks A. C., 1986, ApJ, 303, 401
 Lauroesch J. T., Meyer D. M., Blades J. C., 2000, ApJ, 543, L43
 Millar T. J., Farquhar P. R. A., Willacy K., 1997, A&AS, 121, 139
 Morton D. C., 1991, ApJS, 77, 119
 Penprase B. E., 1993, ApJS, 88, 433
 Péquignot D., Aldrovandi S. M. V., 1986, A&A, 161, 169
 Price R. J., Crawford I. A., Barlow M. J., 2000, MNRAS, 312, L43
 Savage B. D., Bohlin R. C., Drake J. F., Budich W., 1977, ApJ, 216, 291
 Shortridge K. et al., 1998, Starlink User Note, 86.16
 Sofia U. J., Cardelli J. A., Guerin K. P., Meyer D. M., 1997, ApJ, 482, L105
 Spitzer L., 1978, Physical Processes in the Interstellar Medium. John Wiley, New York
 van Dishoeck E. F., 1988, in Millar T. J., Williams D. A., eds, Rate Coefficients in Astrochemistry. Kluwer, Dordrecht, p. 49
 van Dishoeck E. F., Black J. H., 1986, ApJS, 62, 109
 Wardle M., Walker M., 1999, ApJ, 527, L109
 Welty D. E., Fitzpatrick E. L., 2001, ApJ, 551, L175
 Welty D. E., Hobbs L. M., Kulkarni V. P., 1994, ApJ, 436, 152

This paper has been typeset from a TeX/LaTeX file prepared by the author.